

Phosphorylation of the acyl-CoA binding pocket of the FadR transcription regulator in *Sulfolobus acidocaldarius*

Maklad, Hassan R; Gutierrez, Gustavo J; Esser, Dominik; Siebers, Bettina; Peeters, Eveline

Published in:
Biochimie

DOI:
[10.1016/j.biochi.2020.05.007](https://doi.org/10.1016/j.biochi.2020.05.007)

Publication date:
2020

License:
CC BY-NC-ND

Document Version:
Accepted author manuscript

[Link to publication](#)

Citation for published version (APA):

Maklad, H. R., Gutierrez, G. J., Esser, D., Siebers, B., & Peeters, E. (2020). Phosphorylation of the acyl-CoA binding pocket of the FadR transcription regulator in *Sulfolobus acidocaldarius*. *Biochimie*, 175, 120-124. <https://doi.org/10.1016/j.biochi.2020.05.007>

Copyright

No part of this publication may be reproduced or transmitted in any form, without the prior written permission of the author(s) or other rights holders to whom publication rights have been transferred, unless permitted by a license attached to the publication (a Creative Commons license or other), or unless exceptions to copyright law apply.

Take down policy

If you believe that this document infringes your copyright or other rights, please contact openaccess@vub.be, with details of the nature of the infringement. We will investigate the claim and if justified, we will take the appropriate steps.

26 **Highlights**

- 27 • FadR is phosphorylated within its acyl-CoA-binding pocket
- 28 • The eukaryotic-type kinase ArnC phosphorylates FadR *in vitro* at threonine 134
- 29 • The phosphomimetic mutant of FadR is less sensitive for acyl-CoA
- 30 • FadR phosphorylation may control metabolism and chromatin conformation

31

32 **Abstract**

33 The archaeal model organism *Sulfolobus acidocaldarius* possesses a TetR-like transcription
34 factor that represses a 30-kb gene cluster encoding fatty acid metabolism enzymes. Interaction
35 of this regulator, FadR, with acyl-CoA molecules causes a DNA dissociation, which may lead
36 to a derepression of the gene cluster. Previously, a phosphoproteome analysis revealed the
37 phosphorylation of three consecutive amino acids in the acyl-CoA ligand binding pocket. Here,
38 we study this phosphorylation event and show that ArnC, a Hanks-type protein kinase, targets
39 a threonine within the phosphoacceptor motif *in vitro*. Electrophoretic mobility shift assays
40 using a phosphomimetic mutant of FadR demonstrate that the presence of negatively charged
41 groups on the phosphoacceptor motif causes an inhibition of the ligand binding that
42 desensitizes the responsiveness of the regulator to acyl-CoA molecules. Based on these
43 observations, we propose a model in which phosphorylation of FadR in its ligand-binding
44 pocket acts as an additional regulatory layer silencing acyl-CoA responsive derepression of
45 fatty acid and lipid degradation. Moreover, given the recently discovered interplay between
46 FadR and the chromosome structuring protein Coalescin, FadR phosphorylation could also
47 influence local chromosome conformation under specific cellular conditions.

48

49 **Keywords**

50 protein phosphorylation – transcription factor – FadR – *Sulfolobus* – archaea – acyl-CoA

51 **1. Introduction**

52 Protein phosphorylation is an abundant posttranslational modification in the thermoacidophilic
53 crenarchaeon *Sulfolobus acidocaldarius* and the related species *Saccharolobus solfataricus*,
54 as evidenced by phosphoproteomics [1,2]. About ten kinases have been identified in *S.*
55 *acidocaldarius*, belonging to the families of the typical eukaryotic-like Hanks-type protein
56 kinases (ePK) or of the atypical protein kinases (aPK) [3]. Collectively, these kinases are
57 responsible for the phosphorylation of a large number of target proteins: at least 801 unique
58 phosphoproteins, belonging to various functional classes, including 18 transcription regulators
59 [2,3]. This suggests that direct phosphorylation of single-component transcription regulators
60 constitutes an important signal transduction mechanism in *S. acidocaldarius*, especially given
61 the complete absence of two-component systems in Crenarchaeota [3], which are regarded
62 as the bacterial paradigm of phosphorylation-mediated transcription regulation. With the
63 exception of phosphorylation of regulators acting on the expression of the archaeellum [4], the
64 archaeal motility structure, and on biofilm formation in *S. acidocaldarius* [5], very little is
65 currently known about the functional role of phosphorylation of single-component regulators in
66 this organism.

67 Archaea harbor typical bacterial-like transcription regulators [6], exemplified by the TetR-family
68 regulator FadR_{Sa} in *S. acidocaldarius* [7]. FadR_{Sa} is a transcriptional repressor of genes
69 involved in lipid and fatty acid catabolism. In response to interacting with long-chain acyl-CoA
70 molecules, the regulator dissociates from DNA resulting in a derepression. FadR_{Sa} is capable
71 of exerting long-range repressive effects on a 30-kb gene cluster comprising 23 genes by
72 binding to only four genomic binding sites, in contrast to bacterial TetR-family FadR regulators,
73 for which such a regulatory mechanism has never been observed [7]. Although the exact
74 underlying mechanism is unknown, a correlation between binding of FadR_{Sa} and of the
75 chromosome structuring factor coalescin has been observed [8], which may explain such a
76 global mode of repression. In the phosphoproteomics reported in [2], FadR_{Sa} was found to be
77 phosphorylated. Here, we report on the impact of phosphorylation on FadR_{Sa} function and
78 discuss how this process may impact the regulation of fatty acid and lipid metabolism in *S.*
79 *acidocaldarius* and possibly even chromosome organization.

80

81 **2. Materials and methods**

82 **2.1 Cloning, site-directed mutagenesis and protein purification**

83 Kinase genes *Saci_0965*, *Saci_1193* (*arnC*) and *Saci_1694* (*arnD*) were PCR-amplified from
84 genomic DNA of *S. acidocaldarius* and cloned into pET28b plasmid vector using the restriction
85 sites NdeI/BamHI (*Saci_0965*), NheI/HindIII (*arnC*) and NdeI/EcoRI (*arnD*), respectively,
86 enabling expression of N-terminally His-tagged proteins. Kinase gene *Saci_1041* was cloned
87 into the vector pET-DueT-1, omitting the transmembrane domains by PCR to improve protein

88 solubility. To generate a triple phosphomimetic mutant (Y¹³³D-T¹³⁴E-T¹³⁵E) of FadR_{Sa},
89 FadR_{Sa}^{PM}, site-directed mutagenesis of the *fadR_{Sa}* coding region was performed with the
90 overlap PCR mutagenesis approach [9] using pET24ax_{fadR_{Sa}}*Ndenu11* [7] as a template.
91 Similar as for the wild-type (WT) FadR_{Sa} protein, the resulting construct enables expression of
92 a C-terminally His-tagged recombinant protein. All oligonucleotides, plasmids and strains used
93 in this work are provided in **Supplementary Tables S1, S2 and S3**, respectively.

94 All recombinant proteins were heterologously expressed in *Escherichia coli* employing the *E.*
95 *coli* strains Rosetta (DE3) (FadR_{Sa}, FadR_{Sa}^{PM}, Saci0965 and ArnD) or BL21 CodonPlus (ArnC).
96 This was followed by purification with an affinity chromatography approach as described [7]
97 with the following exceptions for the kinases Saci0965, ArnC and ArnD: induction of
98 heterologous proteins was performed by adding 1 mM isopropyl β-D-1-thiogalactopyranoside
99 to the cultures at an optical density (OD₆₀₀) of 0.7, followed by overnight incubation at 37°C.
100 The resulting cell extracts were not subjected to heat treatment as was done for FadR_{Sa} and
101 its mutant variant. Saci1041 was, after dialysis against 20 mM Tris-HCl [pH 7.0], further
102 subjected to anion exchange chromatography (UNO Q-17) using a linear salt gradient to 1 M
103 NaCl. Subsequently, Saci1041, as well as ArnC and ArnD, were further purified using a size
104 exclusion chromatography step with a HiLoad® Superdex 200 16/60 column and an ÄKTA
105 Fast Protein Liquid Chromatography (FPLC) system (GE Healthcare Life Sciences). All protein
106 preparations with the exception of Saci1041 were ultimately dialyzed using storage buffer (20
107 mM Na₂HPO₄/NaH₂PO₄ [pH 7.4], 0.5 M NaCl). The Saci1041 preparation was stored in 50 mM
108 Tris-HCl [pH 7.0], 0.3 M NaCl.

109

110 **2.2 *In vitro* phosphorylation assay**

111 Between 0.2 and 4 µg of purified proteins were incubated in a total volume of 30 µl reaction
112 buffer (25 mM Tris-HCl [pH 7.4], 100 mM NaCl, 10 mM MgCl₂ and 1 mM 1,4-dithiothreitol
113 (DTT)) containing 100 µM non-labeled adenosine triphosphate (ATP) and 33 nM (3 µCi) ³²P-
114 γ-ATP (3000 Ci mmol⁻¹, PerkinElmer). Reactions were incubated for 30 minutes at 65°C and
115 stopped by adding 5 µl 4x NuPAGE LDS Sample Buffer (Thermo Fisher Scientific) and by
116 heating at 95°C for 5 minutes. Subsequently, proteins were separated by sodium dodecyl
117 sulfate polyacrylamide gel electrophoresis (SDS-PAGE) and Coomassie-stained.
118 Autoradiograph imaging was performed by drying the gel and employing a Personal Molecular
119 Imager system (Bio-Rad Laboratories).

120

121 **2.3 Mass spectrometry analysis**

122 Experimental procedures for mass spectrometry analyses are provided in **Supplementary**
123 **Materials (Supplementary Methods)**.

124 **2.4 Electrophoretic mobility shift assay**

125 *In vitro* protein-DNA binding assays were performed using ³²P-radiolabeled DNA fragments
126 harboring the *Saci_1106* promoter region [7]. One primer was first labeled with ³²P-γ-ATP
127 (Perkin Elmer) with the help of T4 polynucleotide kinase (Thermo Scientific). A PCR was then
128 performed with the labeled and the non-labeled primers (**Supplementary Table S1**) after
129 which amplified double stranded (ds) DNA fragments were purified by acrylamide gel
130 electrophoresis. Binding assays were done using 4 μg FadR_{Sa} or FadR_{Sa}^{PM} proteins (at a final
131 concentration of 6.8 μM), 1 μl radiolabeled DNA (15000 cpm/μl), and 0.5 μg sonicated salmon
132 sperm DNA as competitor DNA in binding buffer (20 mM Tris-HCl [pH 8.0], 0.1 mM DTT, 1 mM
133 MgCl₂, 12.5% glycerol, 50 mM NaCl, 0.4 mM EDTA). Stearoyl-CoA was added to the reactions
134 in an increasing concentration gradient (between 0.1 and 100 μM), using dimethylsulfoxide as
135 a solvent to dissolve acyl-CoA. Reactions were incubated during 20 minutes at 37°C prior to
136 an electrophoresis on a 6% native polyacrylamide gel. Visualization was achieved by
137 autoradiography and scanning using a Bio-500 Microtek scanner. Integrated densities of free
138 DNA bands were measured using ImageJ (NIH) and the values were normalized taking into
139 account the background and then converted into DNA-bound fractions. The inhibition
140 coefficient (IC₅₀) was calculated using Prism7 (GraphPad) by a non-linear fitting using an
141 inhibitor vs. normalized response equation.

142

143 **3. Results and Discussion**

144 **3.1 FadR_{Sa} is phosphorylated in its ligand-binding pocket *in vivo* and *in vitro***

145 FadR_{Sa} was previously found to be phosphorylated on three consecutive residues, Y¹³³, T¹³⁴
146 and T¹³⁵, in a phosphoproteomic survey [2] (**Figure 1A**). These amino acids are located in the
147 α7 helix within the ligand-binding pocket, as shown in the native FadR_{Sa} crystal structure (PDB
148 5MWR) [7]. This dimeric protein structure is characterized by an asymmetric ligand binding,
149 with lauroyl-CoA present in the ligand-binding pocket of subunit B, but not subunit A [7]. A
150 closer view at the lauroyl-CoA-FadR_{Sa} interactions in subunit B unveils an important role for
151 Y¹³³ in ligand binding at the initial part of the binding cavity, by establishing hydrophobic
152 interactions with the pantothenic acid moiety of lauroyl-CoA and by forming a hydrogen bond
153 with its β-mercapto-ethylamine group. The electron density map [7] indicated that Y¹³³ in
154 subunit A is phosphorylated (**Figure 1B**). This was an unexpected finding, since the protein
155 was heterologously produced in *E. coli* [7]. Upon comparing the Y¹³³ conformation in both
156 subunits in the molecular model, it can be suggested that the presence of a phosphate group
157 on Y¹³³ could prevent Y¹³³-acyl-CoA interactions and that it might even sterically hinder the
158 presence of acyl-CoA in the binding pocket.

159 That hypothesis prompted us to investigate which kinases might be responsible for FadR_{Sa}
160 phosphorylation. A set of four *S. acidocaldarius* kinases (ArnC, ArnD, Saci1041 and Saci0965)
161 were analyzed in an *in vitro* phosphorylation assay, and while all four kinases displayed
162 autophosphorylation signals (**Figure 1C**), only the addition of the ePKs ArnC and Saci1041
163 generated additional phosphorylation signals at the level of FadR_{Sa}. In the autoradiograph, two
164 different bands representing phosphorylated FadR_{Sa} were observed (**Figure 1C**). The lower-
165 MW band (FadR_{Sa}') was not observed in the corresponding Coomassie-stained SDS-PAGE
166 (**Figure 1C**), however, it was observed upon loading higher FadR_{Sa} amounts for
167 electrophoresis (**Supplementary Figure S1**). Mass spectrometry analysis indicated that both
168 bands consisted of full-length FadR_{Sa} protein, suggesting that the lower-MW band represents
169 a conformationally distinct FadR_{Sa} population. Despite that this FadR_{Sa} population represents
170 a minor fraction, the Saci1041 kinase preferentially phosphorylated this conformational state
171 of the protein in contrast to ArnC (**Figure 1C**). Upon evaluating the corresponding Coomassie-
172 stained SDS-PAGE, there were no indications that phosphorylation causes a shift in the
173 relative abundance of these two populations.

174 To identify the phosphorylated FadR_{Sa} residues, the proteins present in the reaction mixtures
175 were subjected to mass spectrometry analysis (**Figure 1A**). After incubating FadR_{Sa} with either
176 ArnC or Saci1041, residues T⁷⁸, T⁸⁰ and T¹¹⁴ were found to be phosphorylated. The first residue
177 T⁷⁸ was also found to be phosphorylated in the non-treated FadR_{Sa} preparation, albeit with low
178 localization probability, demonstrating that this phosphorylation was already present after
179 heterologous expression in *E. coli*. In addition, ArnC targeted T¹³⁴ which is among the *in vivo*
180 phosphorylated tripartite target site. Phosphorylation of Y¹³³, which was reported in the
181 previous phosphoproteome study [2], was not detected in this assay leaving the kinase
182 responsible for the phosphorylation of that tyrosine in FadR_{Sa} unknown.

183

184 **3.2 Phosphomimetic mutation of FadR_{Sa} sites targeted for phosphorylation inhibits** 185 **ligand response**

186 A triple phosphomimetic mutant of FadR_{Sa}, FadR_{Sa}^{PM} (Y¹³³D-T¹³⁴E-T¹³⁵E), was prepared
187 thereby introducing residues with a negative electrostatic potential to mimic the
188 phosphorylation observed *in vivo* [2]. In electrophoretic mobility shift assays (EMSAs), it was
189 observed that FadR_{Sa}^{PM} displays a similar DNA-binding behavior as the WT protein, albeit with
190 a somewhat lower affinity (**Supplementary Figure S2**). Binding of acyl-CoA disrupts FadR_{Sa}-
191 DNA complex formation by altering protein conformation [7]. In testing the hypothesis that
192 phosphorylation inhibits acyl-CoA binding, EMSAs were performed with FadR_{Sa}^{WT} and
193 FadR_{Sa}^{PM} (**Figure 2**). Whereas the addition of the long-chain acyl-CoA stearoyl-CoA abrogated
194 DNA binding of FadR_{Sa}^{WT} at low concentrations (starting at 0.3 μM), FadR_{Sa}^{PM} was clearly less
195 responsive with an inhibition coefficient (IC₅₀) being about 56 times higher (**Figure 2**).

196 FadR_{Sa}^{PM}-DNA complexes were therefore more resistant to disruption even at high acyl-CoA
197 concentrations, suggesting that phosphorylation in the ligand-binding pocket renders FadR_{Sa}
198 insensitive to acyl-CoA binding.

199

200 **4. Conclusions**

201 FadR_{Sa} is phosphorylated *in vitro* by two kinases, ArnC and Saci1041, with ArnC targeting a
202 threonine in a three-residue stretch previously found to be phosphorylated *in vivo* [2] and
203 located at the initial entry section of the acyl-CoA binding cavity. ArnC is considered to be a
204 globally acting kinase in *S. acidocaldarius*, a master regulatory kinase in the archaeal
205 regulatory network [10] and capable of phosphorylating almost all other kinases as shown in
206 the related *Sulfolobus islandicus* [11]. It is unknown which kinase(s) target(s) Tyr¹³³, which is
207 ideally positioned to inhibit ligand binding upon phosphorylation as shown in the FadR_{Sa} crystal
208 structure [7]. Of note, a tyrosine kinase has not yet been identified in archaea [3]. Nevertheless,
209 the observation that a phosphomimetic mutant of FadR_{Sa} is less responsive to acyl-CoA *in*
210 *vitro* strongly suggests that phosphorylation of this site *in vivo* acts as a signal to switch off
211 ligand response of the regulator, resulting in a continuous repression of genes encoding lipid
212 and fatty acid degradation. Given the interplay between FadR_{Sa} and the chromosome-
213 structuring factor coalescin [8], phosphorylation of the FadR_{Sa} ligand-binding pocket could thus
214 lead to maintaining a large 30-kb genomic region in a condensed and transcriptionally
215 repressed state, regardless of intracellular acyl-CoA concentrations. Phosphorylation-
216 mediated inhibition of ligand binding emerges as a unique mechanism not observed before for
217 prokaryotic TetR-family regulators. Instead, bacterial single-component regulators are more
218 commonly found to be phosphorylated in the helix-turn-helix domain thereby inhibiting DNA
219 binding [12].

220

221 **Figure captions**

222 **Figure 1. FadR_{Sa} is phosphorylated in its acyl-CoA binding pocket. A.** Secondary structure
223 map of FadR_{Sa} showing domain organization. Phosphorylated residues, observed *in vivo* [2]
224 or *in vitro* by mass spectrometry analysis are indicated in a table, with their locations also
225 annotated on the secondary structure map. The asterisk indicates that the phosphorylation
226 was detected with low localization probability and that it only occurred on one of these possible
227 residues. **B.** Cartoon representation of the FadR_{Sa} crystal structure (PDB 5MWR) [7] with
228 indication of the phosphorylated tyrosine (pY¹³³) modeled in subunit A in a colored ball-and-
229 stick representation, as well as a heptanoyl-CoA ligand modeled in subunit B. Zooms are
230 presented for the ligand-binding pocket of each subunit. **C.** *In vitro* phosphorylation assay
231 testing phosphorylation of FadR_{Sa} by various *S. acidocaldarius* kinases. Following protein
232 concentrations were used in the assay: 2.30 μM (FadR_{Sa}), 0.51 μM (ArnC), 2.55 μM

233 (Saci0965), 0.70 μ M (ArnD) and 0.08 μ M (Saci1041). The Coomassie-stained SDS-PAGE and
234 autoradiographs are aligned to each other, with the two last lanes being displayed using the
235 same autoradiograph but at a longer exposure time. Two electrophoretically different FadR_{Sa}
236 species are annotated as FadR_{Sa} and FadR_{Sa}', respectively, with the second species not
237 being visible in the SDS-PAGE (see also **Supplementary Figure S1**). The assay was
238 performed three times with similar results. Only one of the assays is shown as a representative
239 result.

240

241 **Figure 2. The FadR_{Sa}^{PM} mutant protein is less sensitive to acyl-CoA binding *in vitro* than**
242 **the WT protein.** Representative autoradiographs of electrophoretic mobility shift assays
243 (EMSAs) of the binding of FadR_{Sa}^{WT} (**A**) and FadR_{Sa}^{PM} (**B**) to a 154-bp DNA fragment
244 representing the operator/promoter region of the *Saci_1106* target gene in the presence of
245 increasing stearyl-CoA concentration. Calculated inhibition coefficient (IC₅₀) values, based on
246 three replicate EMSAs, are displayed next to the autoradiographs.

247

248 **Acknowledgements**

249 We are grateful to Julia Reimann and Sonja-Verena Albers for the construction of pSVA1011.
250 We thank Francis Impens (VIB Proteomics Expertise Center) for performing the LC-MS/MS
251 analysis and Karl Jonckheere for technical assistance with protein purification.

252

253 **Funding sources**

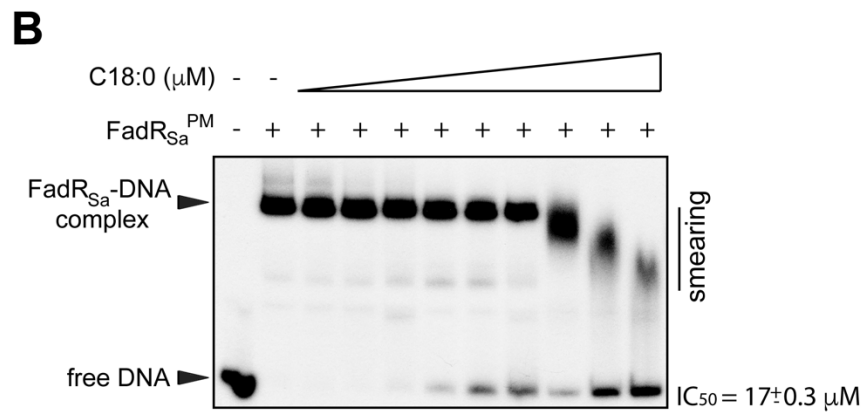
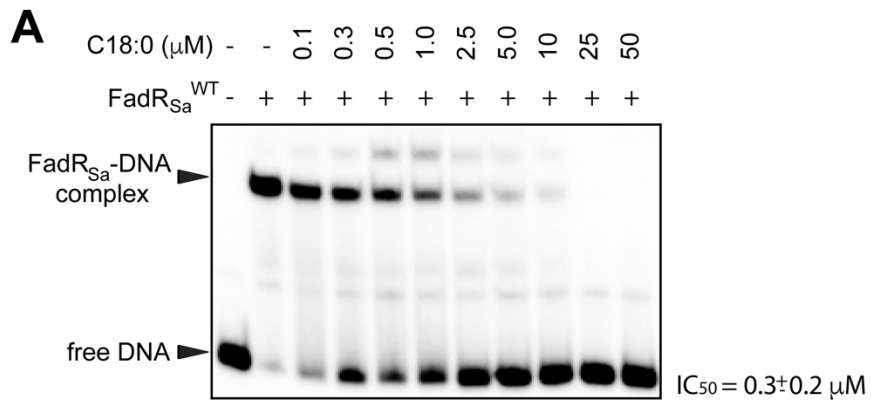
254 This work was supported by the Research Council of the Vrije Universiteit Brussel and by the
255 Research Foundation Flanders (FWO-Vlaanderen) [research grant 1526418N and research
256 project G021118].

257

258 **References**

- 259 [1] D. Esser, T.K. Pham, J. Reimann, S. V. Albers, B. Siebers, P.C. Wright, Change of
260 carbon source causes dramatic effects in the phosphoproteome of the archaeon
261 *Sulfolobus acidocaldarius*, J. Proteome Res. 11 (2012) 4823-4833.
- 262 [2] J. Reimann, D. Esser, A. Orell, F. Amman, T.K. Pham, J. Noirel, et al., Archaeal signal
263 transduction: impact of protein phosphatase deletions on cell size, motility, and energy
264 metabolism in *Sulfolobus acidocaldarius*, Mol. Cell Proteomics. 12 (2013) 3908–3923.
- 265 [3] D. Esser, L. Hoffmann, T.K. Pham, C. Bräsen, W. Qiu, P.C. Wright, et al., Protein
266 phosphorylation and its role in archaeal signal transduction, FEMS Microbiol. Rev. 40
267 (2016) 625–647.

- 268 [4] L. Hoffmann, A. Schummer, J. Reimann, M.F. Haurat, A.J. Wilson, M. Beeby, et al.,
269 Expanding the archaeellum regulatory network - the eukaryotic protein kinases ArnC and
270 ArnD influence motility of *Sulfolobus acidocaldarius*, *MicrobiologyOpen*, 6 (2017).
- 271 [5] L. Li, A. Banerjee, L.F. Bischof, H.R. Maklad, L. Hoffmann, A.-L. Henche, et al., Wing
272 phosphorylation is a major functional determinant of the Lrs14-type biofilm and motility
273 regulator AbfR1 in *Sulfolobus acidocaldarius*, *Molecular Microbiology*. 105 (2017) 777–
274 793.
- 275 [6] L. Lemmens, H.R. Maklad, I. Bervoets, E. Peeters Transcription regulators in archaea:
276 homologies and differences with bacterial regulators. *J. Mol. Biol.* 431 (2019) 4132-
277 4146.
- 278 [7] K. Wang, D. Sybers, H.R. Maklad, L. Lemmens, C. Lewyllie, X. Zhou et al, A TetR-family
279 transcription factor regulates fatty acid metabolism in the archaeal model organism
280 *Sulfolobus acidocaldarius*, *Nat. Communications* 10 (2019) 1542.
- 281 [8] N. Takemata, R.Y. Samson, S.D. Bell, Physical and functional compartmentalization of
282 archaeal chromosomes, *Cell* 179 (2019) 165-179.
- 283 [9] R. Higuchi, B. Krummel, R.K. Saiki, A general method of *in vitro* preparation and specific
284 mutagenesis of DNA fragments: study of protein and DNA interactions, *Nucleic Acids*
285 *Res.* 16 (1988) 7351–7367.
- 286 [10] L. Hofmann, A. Schummer, J. Reimann, M.F. Haurat, A.J. Wilson, M. Beeby, W.
287 Warscheid, S.-V. Albers, Expanding the archaeellum regulatory network – the eukaryotic
288 protein kinases ArnC and ArnD influence motility of *Sulfolobus acidocaldarius*,
289 *MicrobiologyOpen* 6 (2017) e00414.
- 290 [11] Q. Huang, Q. Zhong, J.B.A. Mayaka, J. Ni, Y. Shen, Autophosphorylation and cross-
291 phosphorylation of protein kinases from the crenarchaeon *Sulfolobus islandicus*. *Front.*
292 *Microbiol.* 8 (2017) 2173.
- 293 [12] A. Derouiche, V. Bidnenko, R. Grenha, N. Pignonneau, M. Ventroux, M. Franz-Wachtel
294 et al, Interaction of bacterial fatty-acid-displaced regulators with DNA is interrupted by
295 tyrosine phosphorylation in the helix-turn-helix domain, *Nucleic Acids Res.* 41 (2013)
296 9371-9381.
297



300
301
302

Figure 2

303 **BIOCHIMIE conflict of interest declaration and author agreement form**

304

305 *Title of Paper:* Phosphorylation of the acyl-CoA binding pocket of the FadR transcription
306 regulator in *Sulfolobus acidocaldarius*

307 *Author (s):* Hassan R. Maklad, Gustavo J. Gutierrez, Dominik Esser, Bettina Siebers, Eveline
308 Peeters

309

310 *Please delete one of the following two lines:*

311 We have no conflict of interest to declare.

312

313

314

315

316

317

318 This statement is to certify that all Authors have seen and approved the manuscript being
319 submitted, and agree to the submission to *BIOCHIMIE*. We warrant that the article is the
320 Authors' original work. We warrant that the article has not received prior publication, is not
321 under consideration for publication elsewhere, and will not be submitted for publication
322 elsewhere, in whole or in part, while under consideration for publication in *BIOCHIMIE*. On
323 behalf of all Co-Authors, the corresponding Author shall bear full responsibility for the
324 submission.

325

326 We attest to the fact that all Authors listed on the title page have contributed significantly to
327 the work, have read the manuscript, attest to the validity and legitimacy of the data and their
328 interpretation, and agree to its submission to *BIOCHIMIE*. We further attest that no other
329 person has fulfilled the requirements for authorship as stated in the Elsevier Authorship-
330 factsheet (2017_ETHICS_AUTH02 - attached), but is not included in the list of authors, and
331 that no other person has contributed substantially to the writing of the manuscript but is not
332 included either among the authors or in the acknowledgements.

333

334 All authors agree that no modification to the author list can be made without the written
335 acceptance of all authors and the formal approval of the Editor-in-Chief. All authors accept
336 that the Editor-in-Chief's decisions over acceptance or rejection or in the event of any breach
337 of the Principles of Ethical Publishing in *BIOCHIMIE* being discovered, of retraction are
338 final.

339

340

341 On behalf of all authors (*delete line if not appropriate*)

342

343 *Corresponding Author Signature :*



344

345 *Date* 13/04/2020

346

347

Supplementary Materials

348

Phosphorylation of the acyl-CoA binding pocket of the FadR

349

transcription regulator in *Sulfolobus acidocaldarius*

350

Hassan R. Maklad, Gustavo J. Gutierrez, Dominik Esser, Bettina Siebers and Eveline

351

Peeters

352

353

354 **Supplementary Tables**355 **Supplementary Table S1. Overview of oligonucleotides used in this work.**

Name	Sequence	Purpose
1511	5' -GGGGCTGCAGTCAATGATGGTGATGGTGGTGATGATGGTGATGTGAAAGAATCTGAAC-3'	Cloning truncated gene <i>Saci_1041</i>
1512	5' -GGGCCATGGCATTAAACGAGCTTAGCCTA-3'	Cloning truncated gene <i>Saci_1041</i>
EP323	5' -GGAATTCCATATGTCACGAAACAAAAGG-3'	Cloning <i>Saci_0965</i> (NdeI restriction site)
EP324	5' -CGGGATCCTTAAATTTTAATAAAAACGAGTTAATATTTCCG-3'	Cloning <i>Saci_0965</i> (BamHI restriction site)
EP329	5' -CTAGCTAGCATGGATTTAGCATTC-3'	Cloning <i>Saci_1193</i> (NheI restriction site)
EP330	5' -CCCAAGCTTTTAGATCTCTGAGT-3'	Cloning <i>Saci_1193</i> (HindIII restriction site)
EP333	5' -GGAATTCCATATGGAAAGTAGTAGTG-3'	Cloning <i>Saci_1694</i> (NdeI restriction site)
EP334	5' -GGAATTCTCATTCTTCTCTGCTCT-3'	Cloning <i>Saci_1694</i> (EcoRI restriction site)
EP354	5' -CTTCACTCCAAATCCTATTAGGAAAG-3'	Amplification <i>Saci_1106</i> promoter fragment for EMSA
EP355	5' -GAACTTTATCAGATCAGAATAGACTC-3'	Amplification <i>Saci_1106</i> promoter fragment for EMSA
EP411	5' -GGAATTCCATATGATGTATAGGGCTCC-3'	Cloning <i>fadR_{Sa}^{PM}</i> (NdeI restriction site)
EP412	5' -CCGCTCGAGCCTTGGTGTTAACATATTTTC-3'	Cloning <i>fadR_{Sa}^{PM}</i> (XhoI restriction site)
HM012	5' -CAGAAAGACCTTCTTCATATCTCTCGGCTAGCTTC-3'	Mutagenic primer <i>fadR_{Sa}^{PM}</i>
HM013	5' -GAAGCTAGCCGAGAGAGATGAAGAAGGTCTTTCTG-3'	Mutagenic primer <i>fadR_{Sa}^{PM}</i>

356

357 **Supplementary Table 2. Overview of plasmids used in this work.**

Name	Description/purpose	Reference
pET24a	Protein overexpression vector	Novagen
pET28b	Protein overexpression vector	Novagen
pET-Duet-1	Protein overexpression vector	Novagen
pET24ax <i>fadR_{Sa}Ndenu11</i>	FadR _{Sa} expression vector	[1]
pET24ax <i>fadR_{Sa}^{PM}Ndenu11</i>	FadR _{Sa} ^{PM} expression vector	This work
pET28bx <i>Saci_0965</i>	Saci0965 expression vector	This work
pET28bx <i>arnC</i>	ArnC expression vector	This work
pET28bx <i>arnD</i>	ArnD expression vector	This work
pSVA1011	Saci1041 expression vector	This work

358

359 **Supplementary Table 3. Overview of strains used in this work.**

Name	Description/purpose	Reference or source
<i>Escherichia coli</i> DH5α	Plasmid propagation strain	Gibco
<i>E. coli</i> Rosetta (DE3)	Protein overexpression strain	Novagen
<i>E. coli</i> BL21 (DE3)	Protein overexpression strain	Novagen
<i>E. coli</i> BL21-CodonPlus (DE3)	Protein overexpression strain	Agilent

360 **Supplementary Figures**

361
362

363

364

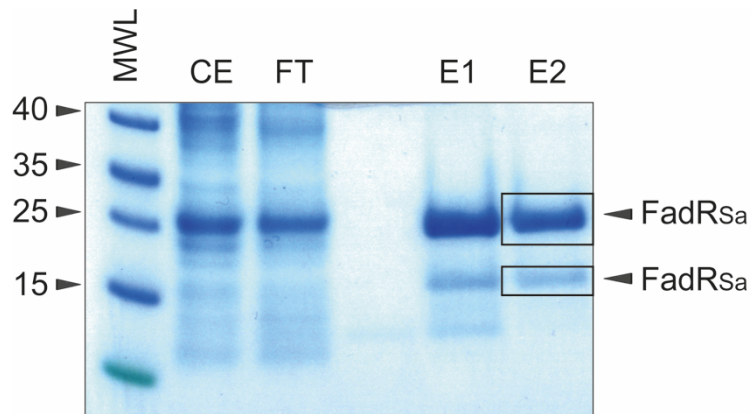
365

366

367

368

369



370

371 **Supplementary Figure S1. Full-length FadR_{Sa} is separated as two electrophoretically distinct populations**

372 **in SDS-PAGE.** Coomassie-stained SDS-PAGE of FadR_{Sa} purification displaying crude extract (CE), flowthrough

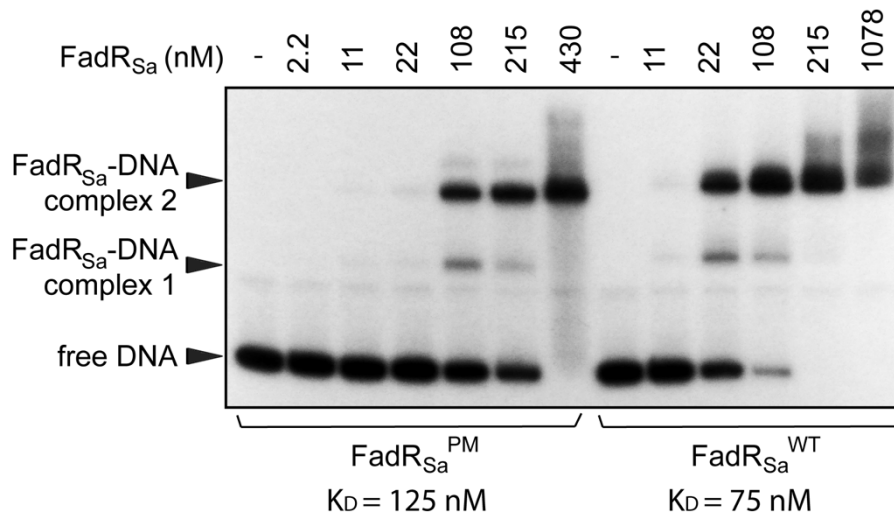
373 (FT) and first and second elution fractions (E1 and E2, respectively). MWL = molecular weight ladder with indication

374 of molecular weights in kDa. The two distinct FadR_{Sa} species that have been subjected to LC-MS/MS analysis after

375 excision from the SDS-PAGE gel are boxed. Both species were shown to contain full-length FadR_{Sa} proteins

376 phosphorylated on T78 or Y79 with low localization probability (see Figure 1A).

377



378
379
380
381
382
383
384
385
386

Supplementary Figure S2. $FadR_{Sa}^{WT}$ and $FadR_{Sa}^{PM}$ have similar DNA-binding behaviours. Autoradiograph of an electrophoretic mobility shift assay (EMSA) of the binding of $FadR_{Sa}^{WT}$ and $FadR_{Sa}^{PM}$ to a 154-bp DNA fragment representing the operator/promoter region of the *Saci_1106* target gene. The calculated dissociation equilibrium constant, calculated based on densitometry of the scanned autoradiograph and fitting to a Hill equation [2], is displayed for both proteins.

387 **Supplementary Methods**

388 **Mass spectrometry analysis**

389 For mass spectrometry analyses, non-radioactive *in vitro* phosphorylation assays were
390 performed using reaction mixtures containing 20 µg FadR_{Sa} and either 2 µg ArnC or 0.2 µg
391 Saci1041 in 30 µl as described above but in a different reaction buffer (25 mM MES [pH 6.5],
392 150 mM KCl, 1 mM MnCl₂ and 0.1 mM ATP) and incubated at 55°C. Proteins were then diluted
393 by adding 70 µl 9 M urea in 20 mM HEPES pH 8.0, reduced by adding 4.5 mM DTT and
394 incubating the mixtures during 30 minutes at 55°C. Alkylation of the proteins was performed
395 by adding 10 mM iodoacetamide and incubating the mixtures during 15 minutes at room
396 temperature in the dark. Samples were subsequently diluted with 100 µl 20 mM HEPES pH
397 8.0 and proteins were digested with 0.4 µg lysyl endopeptidase (Wako, 1/50, w/w) for 4 hours
398 at room temperature. Proteins were further diluted with 200 µl 20 mM HEPES pH 8.0 and
399 digested with 0.1 µg trypsin (Promega, 1/200, w/w) using an overnight incubation at 37°C.
400 Finally, peptides were purified on OMIX C18 pipette tips (Agilent), dried completely by vacuum
401 drying and re-dissolved in loading solvent A (0.1% trifluoroacetic acid (TFA) in
402 water/acetonitrile (98:2, v/v)) for liquid chromatography tandem mass spectrometry (LC-
403 MS/MS) analysis. The details of the LC-MS/MS procedure can be found below.

404 In addition, a sample of FadR_{Sa} was run on SDS-PAGE, leading to the separation of
405 conformationally distinct protein species (**Supplementary Figure S1**), which were excised
406 from the gel after staining, transferred to a tube and immediately cooled using dry ice. Gel
407 bands were then washed with 500 µl H₂O, incubated in 500 µl H₂O/acetonitrile during 15
408 minutes and in 500 µl acetonitrile during another 15 minutes before being dried completely in
409 a vacuum concentrator. Next, 0.15 µg sequencing-grade trypsin (Promega) in 50 mM
410 ammonium bicarbonate in water/acetonitrile (9:1, v/v) was added to the dried gel bands and
411 proteins were digested overnight at 37°C. Peptides eluted from every gel band were dried
412 completely in a vacuum concentrator and re-dissolved in loading solvent A, which were then
413 subjected to LC-MS/MS analysis. The LC-MS/MS procedure is described below.

414 Liquid chromatography tandem mass spectrometry (LC-MS/MS) was performed at the VIB
415 Proteomics Expertise Center. Peptides were injected on an Ultimate 3000 RSLCnano system
416 in-line connected to a Q Exactive mass spectrometer (Thermo). Trapping was performed at 10
417 µl/min for 4 minutes in loading solvent A on a 20 mm trapping column (made in-house, 100 µm
418 internal diameter (I.D.), 5 µm beads, C18 Reprosil-HD, Dr. Maisch, Germany) and the sample
419 was loaded on a 150 mm analytical column (made in-house, 75 µm I.D., 3 µm beads C18
420 Reprosil-HD, Dr. Maisch). Peptides were eluted by a linear increase from 2 to 55% MS solvent
421 B (0.1% FA in water/acetonitrile (2:8, v/v)) over 30 minutes for the gel band samples and over
422 120 minutes for the in-solution samples, all at a constant flow rate of 300 nl/min, followed by a
423 5-minutes wash reaching 99% MS solvent B and re-equilibration with MS solvent A (0.1% FA

424 in water/acetonitrile (2:8, v/v)). The mass spectrometer was operated in data-dependent mode,
425 automatically switching between MS and MS/MS acquisition for the most abundant ion peaks
426 per MS spectrum. Full-scan MS spectra (400-2000 m/z) were acquired at a resolution of
427 70,000 in the orbitrap analyser after accumulation to a target value of 3,000,000. Depending
428 on the instrument settings, the 5 or 10 most intense ions above a threshold value of 13,000 or
429 17,000 were isolated (window of 2.0 Th) for fragmentation at a normalized collision energy of
430 25% after filling the trap at a target value of 50,000 for maximum 80 or 60 ms. MS/MS spectra
431 (200-2000 m/z) were acquired at a resolution of 17,500 in the orbitrap analyser.
432 Data analysis was performed with MaxQuant (version 1.5.3.8) using the Andromeda search
433 engine with default search settings including a false discovery rate set at 1% on both the
434 peptide and protein level. Spectra were searched against the *Escherichia coli* strain K12
435 proteins in the SwissProt database (database release version of May 2016 containing 4,306
436 protein sequences downloaded from www.uniprot.org) supplemented with FadR_{Sa}, ArnC and
437 Saci1041 sequences (Q4J9S1, Q4J9J0 and Q4J9X9, respectively). The mass tolerance for
438 precursor and fragment ions was set to 4.5 and 20 ppm, respectively, during the main search.
439 Enzyme specificity was set as C-terminal to arginine and lysine (trypsin), also allowing
440 cleavage at arginine/lysine-proline bonds with a maximum of two missed cleavages.
441 Carbamidomethylation of cysteine was set as a fixed modification for the in-solution samples
442 only and variable modifications were set to oxidation of methionine residues (to sulfoxides),
443 acetylation of protein N-termini and phosphorylation of serine, threonine and tyrosine residues.
444
445

446 **Supplementary References**

- 447 [1] K. Wang, D. Sybers, H.R. Maklad, L. Lemmens, C. Lewyllie, X. Zhou et al, A TetR-family transcription factor
448 regulates fatty acid metabolism in the archaeal model organism *Sulfolobus acidocaldarius*, Nat
449 Communications 10 (2019) 1542.
450
451 [2] E. Peeters, C. Wartel, D. Maes and D. Charlier. Analysis of the DNA-binding sequence specificity of the
452 archaeal transcriptional regulator Ss-LrpB from *Sulfolobus solfataricus* by systematic mutagenesis and high
453 resolution contact probing, Nucleic Acids Res 35 (2007) 623.
454
455

456

457